Supplementary Information

Buser et al.

SI Materials and Methods

cDNAs and Plasmids. A plasmid encoding the anti-GFP nanobody (NSlmb-vhhGFP4; 1, 2) was provided by E. Caussinus and M. Affolter (Biozentrum, University of Basel). Plasmids encoding siRNA-resistant AP-1γ-FKBP (pLXIN-Ap1g1-FKBP, Addgene plasmid #46946) and Mitotrap (pEYFP-Mitotrap, Addgene plasmid #46942) were provided by M.S. Robinson (CIMR, Cambridge, UK; 3), the plasmid encoding EGFP-CIMPR (pCIpreEGFP-CIMPRtail) by B. Hoflack and M. Anitei (TU Dresden, Germany; 4), a plasmid of BirA from Dietmar Schreiner (Medizinische Hochschule Hannover, Germany). pcDNA3-APEX2-NES (Addgene plasmid #49386) was a gift from A. Ting (MIT, Cambridge, USA), and pRK1043 encoding MBP-TEV (Addgene plasmid #8835) from D. Waugh (NCI, Frederick, MD), pQCXIB w297-1 (Addgene plasmid #22800) was a gift from E. Campeau (University of Massachusetts, Worcester, USA), pQCXIH and pQCXIP were purchased from Takara Bio.

DNA constructs were generated using polymerase chain reaction (PCR) and synthetic oligonucleotides (Microsynth, Balgach, Switzerland) and verified by sequencing. Resulting protein sequences are shown in Supplementary Tables S1–S3.

Bacterial Expression and Purification of Functionalized Nanobodies. Derivatized VHH nanobodies and myc-BirA were cloned into pET-24a and pET-21d (Merck), respectively, transformed together into Rosetta DE3 cells (Merck), and plated on LB plates with 50 μg/ml kanamycin and 50 μg/ml carbenicillin. A 20-ml overnight culture of a single colony was diluted into 1 l LB medium with antibiotics and 200 μM d-biotin and grown to an OD_{600} of 0.6-0.7 at 37°C. Expression was induced with 1 mM isopropyl-β-d-thiogalactopyranosid (IPTG) at 16°C overnight (VHH-mCherry), at 20°C overnight (VHH-APEX2), or at 30°C for 4 h (all other nanobodies). For APEX2-nanobody derivatives, the LB medium was additionally complemented with 1 mM 5-aminolevulinic acid hydrochloride to promote heme incorporation as previously described (5). Cells were pelleted at 5'000×g at 4°C for 45 min and stored at –80°C. Upon thawing, they were resuspended in 30 ml PBS with 20 mM imidazole, 200 μg/ml lysozyme, 20 μg/ml DNase I, 1 mM $MgCl_2$, and 1 mM PMSF, incubated for 10 min at room temperature and 1 h at 4°C while rotating, followed by mechanical lysis using a tip sonicator for 3 times 30 s with 1-min cooling periods. The lysate was cleared by centrifugation at 15'000×g for 1 h at 4°C and loaded on a His GraviTrap column (GE Healthcare Life Sciences), washed with 20 mM imidazole in PBS, and eluted with 2 ml PBS with 500 mM imidazole. The purified nanobodies were desalted on PD-10 columns (GE Healthcare Life Sciences), concentrated to 2 mg/ml (5 mg/ml for VHH-mCherry and -APEX2), flash-frozen in liquid nitrogen, and stored at –80°C. MBP-tagged TEV protease subcloned into pET24a was similarly expressed (4 h induction at 30°C) and isolated. Plasmids for nanobody fusion protein expression are deposited with Addgene (#109417–109424).

Cell Culture and Retroviral Transduction. HeLa α cell lines were maintained in high-glucose Dulbecco's modified Eagle's medium (DMEM) with 10% fetal calf serum (FCS), 100 units/ml streptomycin, 2 mM L-glutamine and appropriate selection antibiotics (1.5 μg/ml puromycin, 1 mg/ml hygromycin B, or 7.5 μg/ml blasticidin) at 37°C in 7.5% CO_2.

Phoenix Ampho packaging cells (from the Nolan lab, Stanford University) were grown in complete medium supplemented with 1 mM sodium pyruvate and transfected with Retro-X Q vectors pQCXIP (resistance for puromycin), pQCXIH (hygromycin B), or pQCXIB (blasticidin) using FuGENE HD (Promega). The viral supernatant was harvested after 48-72 h, passed through a 0.45 μm filter, supplemented with 15 μg/ml polybrene, and added to target HeLa α cells. The next day, complete medium with the antibiotic was added.

HeLa cells stably expressing EGFP reporters (using pQCXIP) were subjected to cell sorting on a FACSAria III (BD Biosciences) to obtain a cell pool with homogenous expression levels. To generate HeLa-AP1ks cell lines, the Mitotrap sequence (Tom70-FRB-3xFLAG) in pQCXIH and γ-FKBP in pQCXIP were transduced into HeLa a cells. Individual clones were analyzed for protein expression and the ability to sequester γ-FKBP to mitochondria upon rapamycin treatment. In addition, EGFP-CDMPR and EGFP-CIMPR were also subcloned into pQCXIB to establish HeLa-AP1ks cells stably expressing these reporters.

RNA Interference and DNA Transfections. For RNA interference, cells were reverse-transfected with target siRNA in Opti-MEM I using Lipofectamine RNAiMAX (both Thermo Fisher Scientific) following the manufacturer's instructions. To silence γ-adaptin in HeLa-AP1ks cells, the siRNA sequence 5'-GAAGAUAGAAUUCACCUUUUU-3' was used as previously described (3). Cells were transfected twice (day 1 and 3) and used at day 5. We used the non-targeting siRNA 5'-UAAGGCUAUGAAGAGAUACdTdT-3' for control knockdowns (6). siRNAs were used at a final concentration of 100 nM and were purchased from Microsynth.

Uptake of Functionalized Nanobodies. Cells were grown in complete medium in 30-mm dishes at 37°C in the CO_2 incubator. At time zero, the medium was supplemented with ~100 nM purified nanobody(e.g. 2 μg/ml VHH-std or VHH-2xTS; 5 μg/ml VHH-mCherry or VHH-APEX2). Uptake was stopped on ice by five washes with ice-cold PBS. Cells were then lyzed with lysis buffer (PBS containing 1% Triton X-100, 0.5% deoxycholate, 2 mM PMSF, and protease inhibitor cocktail), nuclei pelleted by centrifugation at 20'000×g for 15 min, and protein concentration of the lysates measured using the BCA assay and adjusted accordingly. The samples were

www.pnas.org/cgi/doi/10.1073/pnas.1801865115

analyzed by SDS-gel electrophoresis and immunoblotting. For a recycling experiment, cells loaded with VHH-tev nanobodies were washed to remove free nanobody and provided with fresh complete medium containing 100 μg/ml (~2 μM) purified MBP-TEV protease for different times.

To distinguish intracellular from surface localization, cells with VHH-tev bound at 4°C for 30 min or internalized at 37°C were shaved with or without 100 μg/ml (~2 μM) purified MBP-TEV in 50 mM HEPES, pH 7.0, 10 mM EDTA for 2 h at 4°C. Alternatively, the surface was shaved with 1 mg/ml proteinase K (Roche) in PBS with 0.5 mM EDTA for 30 min at 4°C. The proteases were stopped by addition of 5 mM PMSF, protease inhibitor cocktail, and 4 mg/ml BSA.

Gel Electrophoresis and Immunoblot Analysis. Proteins separated by SDS-gel electrophoresis (5–15% polyacrylamide) were transferred to Immobilon-P[SQ] PVDF membranes (Millipore). After blocking with 5% non-fat dry milk in TBS (50 mM Tris·HCl, pH 7.6, 150 mM NaCl) with 0.1% Tween-20 (TBST) for 1 h, the membranes were probed with primary antibodies in 1% BSA in TBST for 2 h at room temperature or overnight at 4°C, followed by incubation with HRP-coupled secondary antibodies in 1% BSA in TBST for 1 h at room temperature. Immobilon Western Chemiluminescent HRP Substrate (Millipore) was used for detection, a Fusion Vilber Lourmat Imaging System for imaging, and Fiji software for quantitation.

Fluorescence Microscopy. For immunofluorescence staining, cells were grown on glass coverslips, fixed with 3% paraformaldehyde (PFA) for 10 min at room temperature, washed with PBS, quenched with 50 mM NH_4Cl in PBS for 5 min, permeabilized with 0.1% Triton X-100 in PBS for 10 min, blocked with 1% BSA in PBS for 15 min, incubated with primary antibody in BSA/PBS for 2 h, washed, and stained with fluorescent secondary antibodies in BSA/PBS for 1 h. After a 5 min staining with 5 µg/ml DAPI and three washes with PBS, coverslips were mounted in Fluoromount-G (Southern Biotech). Staining patterns were imaged on a Zeiss Point Scanning Confocal LSM700 microscope.

Live Cell Imaging. Cells expressing TfR-EGFP or EGFP-CDMPR were grown in 4-well μ-slides (ibiTreat; ibidi). The medium was replaced with 150 μl complete medium with FCS, but without phenol red. Uptake was initiated by adding 150 μl of the same pre-warmed medium containing 2.5 μg/ml (50 nM) VHH-mCherry. Imaging was performed on an automated inverted widefield microscope FEI More equipped with a sCMOS camera (Hamamatsu ORCA flash 4.0) using a U Plan S Apo 100x NA 1.4 oil objective at 37°C and 5% CO_2. EGFP (mCherry) fluorescence was excited at 470/24 nm using an LED lightsource (SpectraX) and recorded at 517/20 nm with single band pass filters (AHF). mCherry fluorescence was excited at 550/15 nm and recorded at 590/20 nm. Per condition ≥10 fields of view (FOV) with an average of 3–4 cells per FOV were recorded before and after VHH-mCherry addition for 100 frames (EGFP-CDMPR) or 60 frames (TfR-EGFP) every 36 s in both channels.

Image processing was performed in ImageJ. Images were corrected for lateral drift using the MultiStackReg plugin on the EGFP channel and applied also to the mCherry channel. Individual cells were selected manually and their signal intensities measured in both channels across all images. Data analysis was performed in Python. Background and auto-fluorescence signal in the mCherry channel before nanobody addition was subtracted. The mCherry signal was normalized to the EGFP signal to account for intensity fluctuations due to organelle movement, cell contraction, axial drift, illumination instabilities etc. Early time points showing artifacts of medium addition were excluded from further analysis. The resulting uptake curves were individually modeled to a first order kinetic process (assuming two compartments, inside and outside of the cell):

$$I(t) = A \cdot (1 - e^{-k(t+t_0)}),$$

where I(t) is the normalized intensity at time t, and t_0 accounts for the time delay between nanobody addition and the start of recording (7). Each process is described by its rate constant k and saturation amplitude A, while t_0 was treated as a global variable across all cells within an experiment. From the rate constant k, the half-life $\tau_{1/2}$ of the process can be calculated as

$$\tau_{1/2} = -\frac{\ln(0.5)}{k}$$

Time of saturation was defined as $5 \cdot \tau_{1/2}$, where 97% of the reaction is completed. Since this simple 'two compartments' model described the recorded data well, we refrained from modeling further compartments to avoid overfitting. Time lapse images were converted to movies using ImageJ and saved as MP4 movie files using the SaveAsMovie plugin at 5 frames/s.

Sulfation Analysis. To analyze retrograde transport and kinetics of EGFP-labeled reporters to the compartment of sulfation, HeLa cell lines were incubated with 1 ml sulfate-free medium for 1 h at 37°C and 7.5% CO_2 before labeling with sulfate-free medium supplemented with 0.5 mCi/ml [^{35}S]sulfate (Hartmann Analytics) and 2 µg/ml purified VHH-std, -1xTS, or -2xTS for up to 75 min. For BFA experiments, 2 µg/ml BFA from a 5000x stock solution in DMSO or DMSO only was added to this labeling solution. For knocksideways experiments, 500 nM rapamycin from a 2000x stock solution in DMSO, or DMSO alone was added.

After incubation, cells were washed twice with ice-cold PBS, lyzed in 1 ml lysis buffer, and centrifuged at 10'000×g for 15 min at 4°C. A fraction (50–100 μl) of the postnuclear supernatants was used for immunoblot analysis of total cell-associated nanobody and an actin control. The rest was incubated for 1 h at 4°C with 20 μl Ni Sepharose High Performance beads (GE Healthcare Life Sciences) to isolate the nanobodies. Beads were washed three times with lysis buffer containing 20 mM imidazole and boiled in SDS-sample buffer. Nanobodies were analyzed by SDS-gel electrophoresis and autoradiography using BAS Storage Phosphor Screens and a Typhoon FLA7000 IP phosphorimager (GE Healthcare Life Sciences).

Compartment Ablation. To inactivate intracellular compartments by DAB crosslinking, we used a modified protocol

established by Stoorvogel and collaborators (8). Cells stably expressing EGFP reporter proteins were grown in 6-well clusters and incubated in complete DMEM containing 5 μg/ml VHH-APEX2 for 1 h at 37°C to reach steady-state. After three washes with ice-cold PBS, cells were incubated with 1 mg/ml DAB, 0.03% H_2O_2, or both in PBS for 90 min at 4°C in the dark, washed twice with PBS containing 5% BSA and three times with PBS before lysis and immunoblot analysis of marker proteins as above.

Electron Microscopy. To label the retrograde route of EGFP-modified reporters by DAB/peroxidase reaction, cells were grown in 100-mm dishes and incubated with 5 μg/ml VHH-APEX2 for 1 h to reach steady-state. Cells were washed twice with buffer (100 mM sodium cacodylate with 2 mM $CaCl_2$, pH 7.4), fixed in 2% glutaraldehyde in buffer at room temperature for 45 min and further processed with minor modifications according to the protocol by Ting and collaborators (5). Cells were rinsed 5 times 2 min with ice-cold buffer, treated with 20 mM glycine in buffer for 5 min to quench remaining glutaraldehyde, and subsequently rinsed another 5 times 2 min in cold buffer. Freshly prepared and filtered solution of 1 mg/ml DAB tetrahydrochloride was combined with 0.03% H_2O_2 in chilled buffer and added to cells for maximally 60 min. Cells were then rinsed 5 times 2 min with cold buffer. Postfixation staining was performed with 2% (w/v) osmium tetroxide for 1 h in cold buffer. Cells were rinsed 5 times 2 min in cold distilled water and placed in 2% (w/v) uranyl acetate (Electron Microscopy Sciences) in distilled water overnight at 4°C, washed in distilled water at room temperature, carefully scraped off the dish, and centrifuged at 700×g for 1 min. The pellet was dehydrated in a graded ethanol series (20%, 50%, 75%, 90%, 95%, 100%, 100%, 100%, 100%), for 10 min each time, then infiltrated with EMBED-812 (Electron Microscopy Sciences) using 1:1 (v/v) resin and anhydrous ethanol for 1 h, followed by two changes into 100% resin before letting set overnight. Finally, the sample was exchanged once more with 100% resin before transfer to fresh resin and polymerization at 60°C for 48 h. Embedded cell pellets were cut with a diamond knife into 70 nm sections and imaged on a Phillips CM100 electron microscope.

For immunoelectron microscopy, EGFP-modified reporter cell lines were grown in 100 mm culture dishes and incubated with 2 µg/ml VHH-myc for 1 h to reach steady-state. Cells were washed twice with PBS, fixed in 3% formaldehyde and 0.2% glutaraldehyde overnight at 4°C, scraped, pelleted, resuspended, washed three times in PBS, incubated with 50 mM NH_4Cl in PBS for 30 min, washed three times in PBS, dehydrated, and infiltrated with LR-GOLD resin according to the manufacturer's instructions (London Resin, London, UK), which was allowed to polymerize for one day at –10°C. Sections of 60-70 nm were collected on carbon-coated Formvar-Ni-grids, and then incubated overnight with an anti-GFP and anti-myc antibodies that were preconjugated to either 10-nm- or 20-nm-sized gold nanoparticles (Abcam) according to the manufacturer's instructions. Grids were washed five times for 5 min in PBS and five times in H_2O, before staining for 10 min in 4% uranyl acetate and 2 min with lead citrate (Reynolds solution). Sections were viewed with a Phillips CM100 electron microscope.

Differential Centrifugation. Confluent HeLa-AP1ks cells of two 100-mm plates were incubated with complete medium containing 500 nM rapamycin from a 2000x stock in DMSO or carrier DMSO only for 10 min at 37°C in 7.5% CO_2, washed with ice-cold PBS, and incubated in 1 ml homogenization buffer (250 mM sucrose, 20 mM HEPES, pH 7.4, 10 mM KCl, 2 mM $MgCl_2$, 1 mM EDTA, 1 mM EGTA, freshly supplemented with 1 mM DTT, 2 mM PMSF, PIC) either containing rapamycin or DMSO only on a rocking platform at 4°C for 5 min. After gentle scraping, the cell suspension was passed 15 times through a 27-gauge needle and kept on ice for 20 min before centrifugation at 700×g for 5 min to pellet nuclei and unbroken cells. The supernatant was transferred into a new tube and centrifuged at 10'000×g for 5 min to pellet mitochondria from cytosol and membranes. The mitochondrial pellet was washed three times with homogenization buffer and lyzed in 200 μl TBS containing 0.1% SDS, 2 mM PMSF and PIC. The supernatant was ultracentrifuged at 100'000×g to separate membranes from cytosol. The pellet was washed twice with 500 μl homogenization buffer and lyzed like the mitochondrial pellet. Corresponding aliquots of all fractions were analyzed by SDS-gel electrophoresis and immunoblotting

Antibodies. For electron microscopy, rabbit anti-GFP (Abcam #ab6556; 1:100) and rabbit anti-myc (Abcam #ab9106; 1:2000) antibodies were used. For immunofluorescence microscopy, goat anti-α-adaptin (Everest Biotech #EB11875; 1:1000), mouse anti-γ-adaptin (from 100/3 hybridoma; 1:500), mouse anti-CDMPR46 (from Jack Rohrer, 22D4 hybridoma; 1:200), mouse Anti-CIMPR (2G11; Abcam #ab2733, 1:1000), rabbit anti-FLAG (Cell Signaling Technology #2368; 1:500), mouse anti-HA (GeneTex #GTX115044; 1:1000), mouse anti-MTCO2 (Abcam #ab3298; 1:1000), mouse anti-TfR (made from OKT8 hybridoma; 1:1000), and sheep anti-TGN46 (Bio-Rad #AHP500GT; 1:1000) antibodies were used. For immunoblotting, mouse anti-a-adaptin (BD Biosciences #610501; 1:5000), rabbit anti-β-1–4-GalT (Novus Biologicals #NBP1-88654; 1:1000), mouse anti-γ-adaptin (BD Biosciences #610385; 1:5000), mouse anti-γ-adaptin (made from 100/3 hybridoma; 1:5000), rabbit anti-a-mannosidase II (LifeSpan BioSciences #LS-C163982; 1:1000), mouse anti-actin (EMD Millipore #MAB1501; 1:100000), mouse anti-Calnexin (BD Biosciences #610523; 1:2000), mouse anti-CHC17 (made from TD.1 hybridoma; 1:200), rabbit anti-CIMPR (GeneTex #GTX130109; 1:1000), rabbit anti-COXIV (Cell Signaling Technology #4850; 1:2500), mouse anti-FLAG (Cell Signaling Technology #8146; 1:1000), rabbit anti-GAPDH (Cell Signaling Technology #5174; 1:10000), mouse anti-GFP (Sigma-Aldrich #11814460001-Roche; 1:5000), mouse anti-HA (made from 12CA5 hybridoma; 1:10000), rabbit anti-His6 (Bethyl Laboratories #A190-114A; 1:10000), rabbit anti-LAMP1 (Cell Signaling Technology #9091; 1:1000), rabbit anti-phospho S6 (Ser235/236) (Cell Signaling Technology #2211; 1:2500), mouse anti-Rab5 (Cell Signaling

Technology #3547; 1:1000), rabbit anti-S6 (Cell Signaling Technology #2217; 1:2500), rabbit anti-T7 (Bethyl Laboratories #A190-117A; 1:10000), mouse anti-TfR (H68.4) (Thermo Fisher Scientific #13-6890; 1:1000), sheep anti-TGN46 (Bio-Rad #AHP500GT; 1:1000), mouse anti-Tom20 (BD Biosciences #612278; 1:1000), rabbit anti-TPST2 (GeneTex #GTX46685; 1:1000), and mouse anti-vti1a (BD Biosciences #611220; 1:1000) antibodies were used.

As secondary antibodies for immunofluorescence microscopy, A488-labeled donkey anti-mouse (Thermo Fisher Scientific #A-21202; 1:500), A488-labeled donkey anti-rabbit (Thermo Fisher Scientific #A-21206; 1:500), A488-labeled donkey anti-goat (Thermo Fisher Scientific #A-11055; 1:500), A568-labeled donkey anti-mouse (Thermo Fisher Scientific #A-10037; 1:500), A568-labeled donkey anti-rabbit (Thermo Fisher Scientific #A-10042; 1:500), A647-labeled donkey anti-rabbit (Thermo Fisher Scientific #A-31573; 1:500), and Cy3-labeled donkey anti-sheep (Jackson Laboratories #713-165-147; 1:200) immunoglobulin antibodies were used. As secondary antibodies for immunoblotting, HRP-labeled goat anti-rabbit (Sigma-Aldrich #A-0545; 1:10000), goat anti-mouse (Sigma-Aldrich #A-0168; 1:10000), and donkey anti-sheep (Sigma-Aldrich #A-3415; 1:5000) immunoglobulin antibodies were used. To detect biotinylated proteins on blots, Streptavidin-HRP (Thermo Fisher Scientific #434323; 1:10000) was used.

1. Caussinus E, Kanca O, Affolter M (2011) Fluorescent fusion protein knockout mediated by anti-GFP nanobody. Nat Struct Mol Biol 19:117-121.
2. Caussinus E, Kanca O, Affolter M (2013) Protein knockouts in living eukaryotes using deGradFP and green fluorescent protein fusion targets. Current protocols in protein science / editorial board, John E. Coligan ... [et al.] 73:Unit 30 32.
3. Robinson MS, Sahlender DA, Foster SD (2010) Rapid inactivation of proteins by rapamycin-induced rerouting to mitochondria. Developmental cell 18:324-331.
4. Waguri S, et al. (2003) Visualization of TGN to endosome trafficking through fluorescently labeled MPR and AP-1 in living cells. Mol Biol Cell 14:142-155.
5. Lam SS, et al. (2015) Directed evolution of APEX2 for electron microscopy and proximity labeling. Nat Methods 12:51-54.
6. Salazar G, et al. (2009) Hermansky-Pudlak syndrome protein complexes associate with phosphatidylinositol 4-kinase type II alpha in neuronal and non-neuronal cells. J Biol Chem 284:1790-1802.
7. Phair RD, Misteli T (2001) Kinetic modelling approaches to in vivo imaging. Nat Rev Mol Cell Biol 2:898-907.
8. Stoorvogel W, Geuze HJ, Griffith JM, Strous GJ (1988) The pathways of endocytosed transferrin and secretory protein are connected in the trans-Golgi reticulum. J Cell Biol 106:1821-1829.

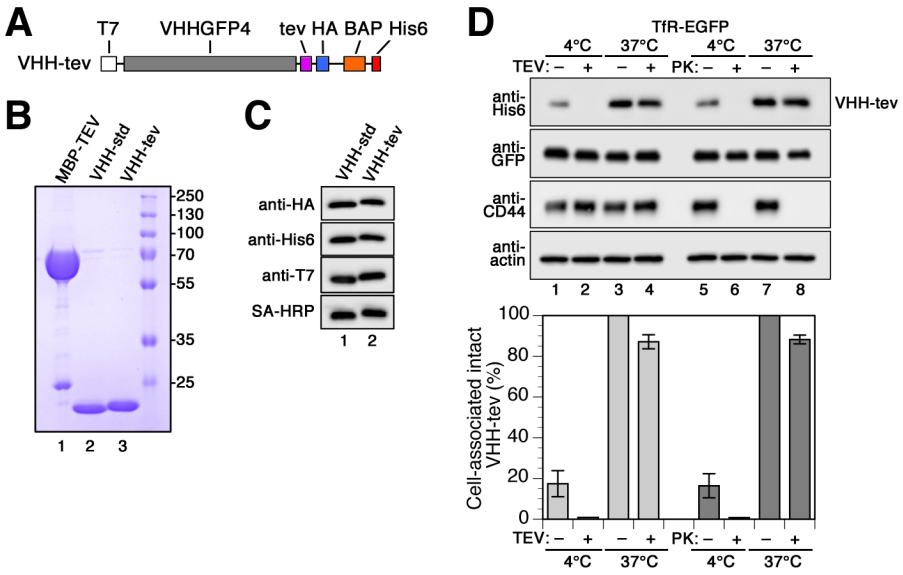

Fig. S1. A derivatized nanobody with a TEV protease cleavage site to monitor recycling to the cell surface.
(A) Schematic representation of the derivatized nanobody containing a cleavage site (tev) for TEV protease. Labeling and scale as in Fig. 1A.
(B) Bacterially expressed and purified maltose-binding protein-TEV protease fusion protein (MBP-TEV; 60 μg) and nanobodies (20 μg) were analyzed by SDS-gel electrophoresis and Coomassie stained. Marker proteins with molecular weights in kDa are shown on the right.
(C) Immunoblot analyses of nanobodies (10 μg) with antibodies against the T7, HA, or His6 epitopes, or with streptavidin-HRP (SA-HRP).
(D) HeLa cells stably expressing TfR-EGFP were incubated with VHH-tev either at 4°C for 30 min or at 37°C for 1 h. After washing cells, TEV protease was added for 2 h at 4°C to remove the C-terminal tags from nanobodies on the surface. Alternatively, the cells were incubated with proteinase K (PK) for 30 min at 4°C to generally digest surface proteins. After inactivation of the protease, cells were lyzed and analyzed by immunoblotting for the nanobody, the reporter, and CD44 as a cell surface marker. Results of protected nanobody were quantified and presented in percent of the value after uptake at 37°C (mean and standard deviation from three independent experiments).

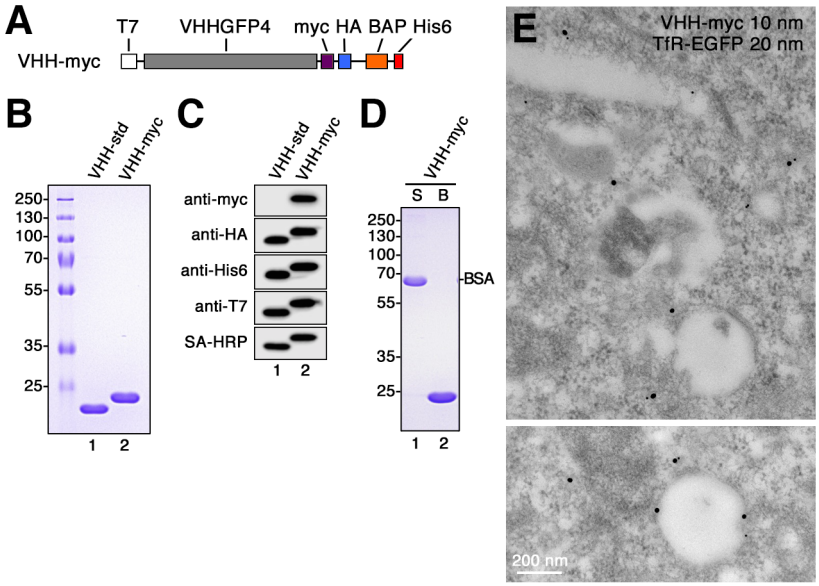

Fig. S2. Immunogold electron microscopy to identify compartments containing nanobodies internalized by an EGFP-tagged reporter protein.
(A) Schematic representation of the derivatized nanobody containing a myc epitope. Labeling and scale as in Fig. 1A.
(B) Bacterially expressed and purified nanobodies (20 μg) were analyzed by SDS-gel electrophoresis and Coomassie stained. Marker proteins with molecular weights in kDa are shown on the left.
(C) Immunoblot analyses of nanobodies (10 μg) with antibodies against the myc, HA, His6, or T7 epitopes, or with streptavidin-HRP (SA-HRP).
(D) Complete biotinylation fpr VHH-myc was confirmed using streptavidin-agarose as in Fig. 1D.
(E) Immunoelectron microscopy of VHH-myc nanobodies internalized for 1 h by cells stably expressing TfR-EGFP. Sections were double-labeled with 10-nm colloidal gold for VHH-myc and 20-nm gold for TfR-EGFP.

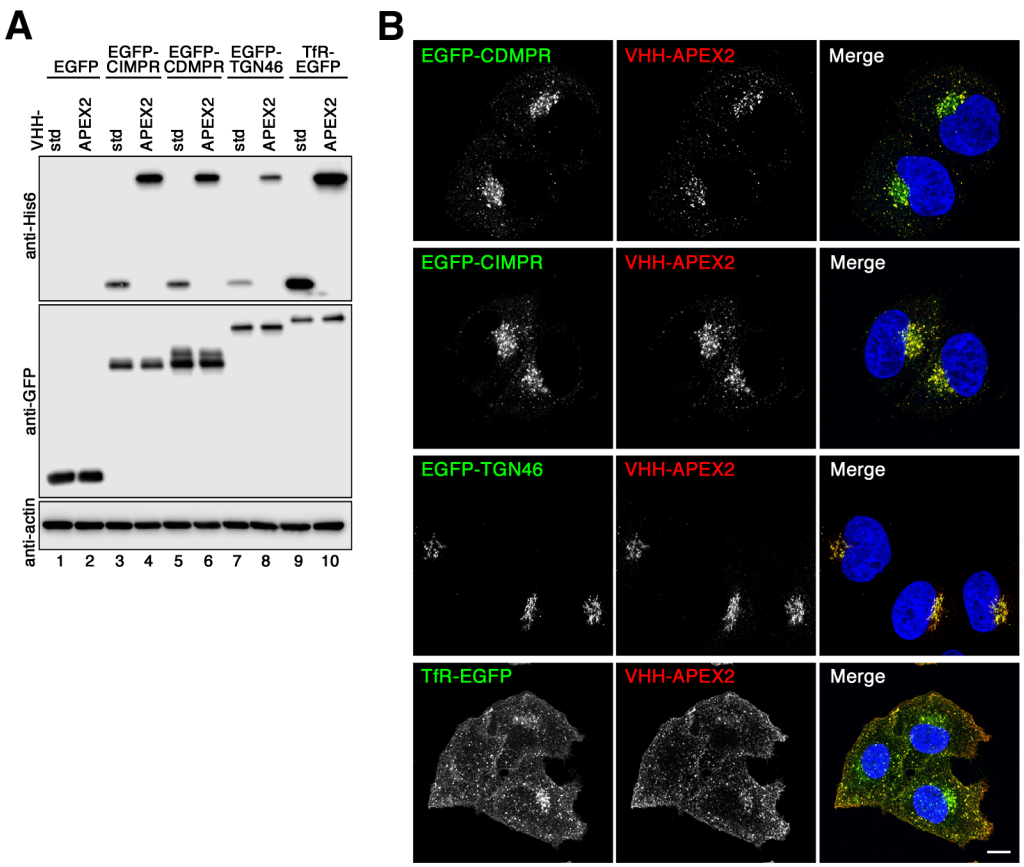

Fig. S3. Endocytic uptake of VHH-APEX2 nanobodies by EGFP-tagged surface proteins
(A) HeLa cells stably expressing cytosolic EGFP or the indicated EGFP fusion proteins were incubated for 1 h at 37°C with 2 μg/ml VHH-std or 5 μg/ml VHH-APEX2 (~0.1 μM), washed, lyzed, and subjected to immunoblot analysis for the nanobodies and the EGFP reporter proteins.
(B) HeLa cell lines expressing EGFP fusion proteins at the cell surface were incubated for 1 h with 5 μg/ml VHH-APEX2, washed, fixed, and imaged by fluorescence microscopy using an anti-HA antibody to detect the nanobodies. Bar: 10 μm.

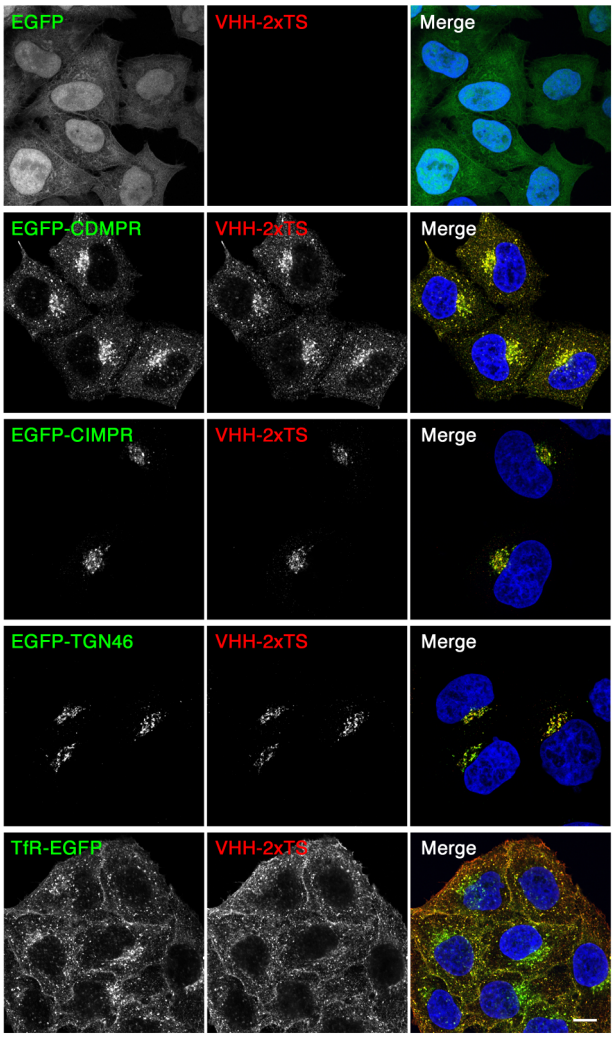

Fig. S4. Endocytic uptake of VHH-2xTS nanobodies by EGFP-tagged surface proteins. HeLa cell lines expressing cytosolic EGFP or the indicated EGFP fusion proteins at the cell surface were incubated for 1 h with 5 μg/ml VHH-2xTS, washed, fixed, and imaged by fluorescence microscopy using an anti-HA antibody to detect the nanobodies. Bar: 10 μm.

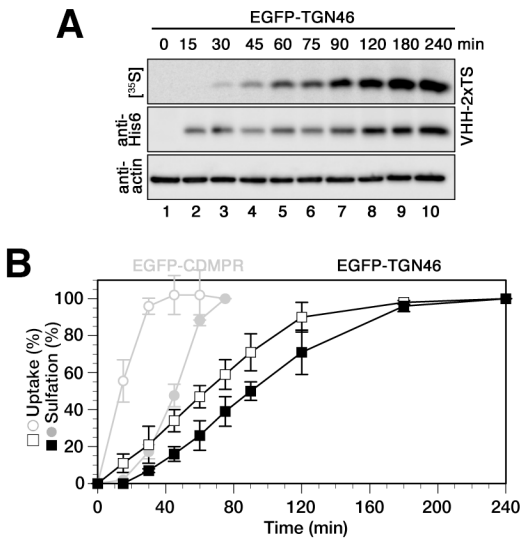

Fig. S5. Retrograde transport of EGFP-TGN46.
(A) HeLa cells stably expressing EGFP-TGN46 were labeled with [^{35}S]sulfate for up to 240 min in the presence of 2 µg/ml VHH-2xTS before analysis as in Fig. 5.
(B) Quantitation of VHH-2xTS uptake (open squares) and sulfation (filled squares) shown in percent of the value after 240 min (mean and standard deviation from three independent experiments). For comparison, the results for uptake and sulfation of VHH-2xTS by EGFP-CDMPR copied from Fig. 5D was superimposed in gray symbols (open for uptake and filled for sulfation). Note that each curve is normalized to 100% for the last data point. Fig. 5A shows that sulfation after 1 h of nanobody uptake by EGFP-TGN46 is higher than by EGFP-CDMPR. The discrepancy most likely reflect the difference of cumulative residence times of nanobodies bound to the two reporters.

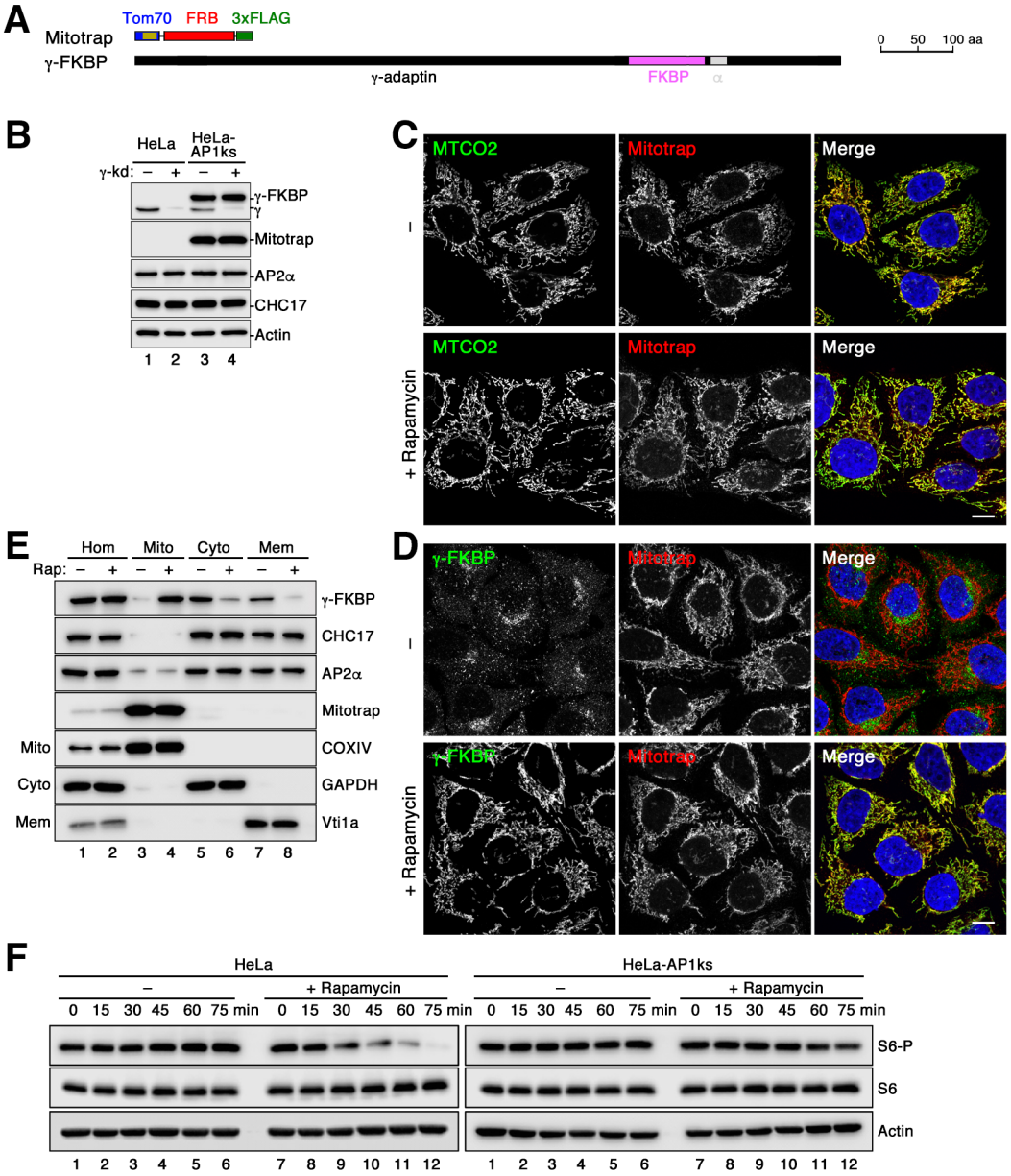

Fig. S6. Characterization of the AP-1 knocksideways cell line.

(A) Mitotrap and γ-FKBP were stably expressed in HeLa cells to generate HeLa-AP1ks for rapid sequestration of AP-1 on mitochondria. As shown schematically, Mitotrap is composed of the signal and transmembrane domain (in blue and yellow) of Tom70p mitochondrial outer membrane protein, the FKBP-rapamycin binding domain (FRB; red) of mTOR, and a 3xFLAG epitope tag (green). γ-FKBP (from 20) consists of FKBP12 (pink) inserted into the hinge region of an siRNA-resistant version γ-adaptin subunit (black) of AP-1 containing a brain-specific α epitope sequence (gray). Scale bar in amino acids (aa).

(B) Lysates of normal HeLa cells and HeLa-AP1ks cells stably expressing γ-FKBP and Mitotrap with or without siRNA-mediated knockdown of the endogenous γ-adaptin were subjected to immunoblot analysis for both forms of γ-adaptin, Mitotrap (anti-FLAG), the α-adaptin subunit of AP-2, and clathrin heavy chain (CHC17). Knockdown efficiencies were typically >85%.

(C and D) After siRNA-mediated silencing of endogenous γ-adaptin, AP-1 knocksideways cells were treated for 10 min with or without 500 nM rapamycin and processed for immunofluorescence microscopy. In panel C, cells were stained for Mitotrap (anti-FLAG) and the mitochondrial marker MTCO2, which perfectly colocalized. In panel D, cells were stained for γ-FKBP (anti-α-epitope) and Mitotrap, demonstrating efficient rapamycin-induced relocalization of AP-1 to mitochondria. Bar: 10 *μ*m.

(E) HeLa-AP1ks cells after knockdown of endogenous γ-adaptin were treated with or without 500 nM rapamycin for 10

min. The postnuclear homogenate (Hom) was separated by differential centrifugation into fractions of mitochondria, other membranes, and cytosol and subjected to immunoblot analysis with antibodies targeting γ-FKBP, CCV coats (clathrin CHC17 and α-adaptin of AP-2), mitochondria (Mitotrap and COXIV), cytosolic glyceraldehyde-3-phosphate dehydrogenase (GAPDH) and the endosomal SNARE protein Vti1a.
(F) Parental HeLa and HeLa-AP1ks cells were treated with or without 500 nM rapamycin for up to 75 min and analyzed by SDS-gel electrophoresis and immunoblotting for phospho-S6, total S6 and actin. TOR inhibition is apparent from the loss of S6 phosphorylation in parental HeLa, but much reduced in HeLa-AP1ks cells.

Movie S1. Live imaging of mCherry-nanobody uptake by EGFP-CDMPR.
HeLa cells stably expressing EGFP-CDMPR were incubated at 37°C in complete medium with 25 nM VHH-mCherry and imaged for EGFP and mCherry fluorescence every 36 s. The movie was rendered at 5 frames/s, corresponding to 3 min/s.

Movie S2. Live imaging of mCherry-nanobody uptake by TfR-EGFP.
HeLa cells stably expressing TfR-EGFP were incubated at 37°C in complete medium with 25 nM VHH-mCherry and imaged for EGFP and mCherry fluorescence every 36 s. The movie was rendered at 5 frames/s, corresponding to 3 min/s.

Table S1: Protein sequences of the functionalized nanobodies used in this study.
T7 epitope in gray, VHH in black, HA epitope in blue, BAP sequence in orange, hexahistidine in red, TEV cleavage site in purple, myc epitope in magenta, the tyrosine sulfation sequence in yellow, APEX2 in green, and mCherry in pink.

Nanobody	Protein sequence
VHH-std	MASMTGGQQMGRGSDQVQLVESGGALVQPGGSLRLSCAASGFPVNRYSMRWYRQAPGKER EWVAGMSSAGDRSSYEDSVKGRFTISRDDARNTVYLQMNSLKPEDTAVYYCNVNVGFEYW GQGTQVTVSSTSEFDYPYDVPDYAGAQPARSGGGLNDIFEAQKIEWHEGALEHHHHHH
VHH-tev	MASMTGGQQMGRGSDQVQLVESGGALVQPGGSLRLSCAASGFPVNRYSMRWYRQAPGKER EWVAGMSSAGDRSSYEDSVKGRFTISRDDARNTVYLQMNSLKPEDTAVYYCNVNVGFEYW GQGTQVTVSSTSENLYFQSEFDYPYDVPDYAGAQPARSGGGLNDIFEAQKIEWHEGALEH HHHHH
VHH-myc	MASMTGGQQMGRGSDQVQLVESGGALVQPGGSLRLSCAASGFPVNRYSMRWYRQAPGKER EWVAGMSSAGDRSSYEDSVKGRFTISRDDARNTVYLQMNSLKPEDTAVYYCNVNVGFEYW GQGTQVTVSSTSEQKLISEEDLEFDYPYDVPDYAGAQPARSGGGLNDIFEAQKIEWHEGA LEHHHHHH
VHH-1xTS	MASMTGGQQMGRGSDQVQLVESGGALVQPGGSLRLSCAASGFPVNRYSMRWYRQAPGKER EWVAGMSSAGDRSSYEDSVKGRFTISRDDARNTVYLQMNSLKPEDTAVYYCNVNVGFEYW GQGTQVTVSSTSSAEDYEYPSEFDYPYDVPDYAGAQPARSGGGLNDIFEAQKIEWHEGAL EHHHHHH
VHH-2xTS	MASMTGGQQMGRGSDQVQLVESGGALVQPGGSLRLSCAASGFPVNRYSMRWYRQAPGKER EWVAGMSSAGDRSSYEDSVKGRFTISRDDARNTVYLQMNSLKPEDTAVYYCNVNVGFEYW GQGTQVTVSSTSSAEDYEYPSAEDYEYPSEFDYPYDVPDYAGAQPARSGGGLNDIFEAQK IEWHEGALEHHHHHH
VHH-APEX2	MASMTGGQQMGRGSDQVQLVESGGALVQPGGSLRLSCAASGFPVNRYSMRWYRQAPGKER EWVAGMSSAGDRSSYEDSVKGRFTISRDDARNTVYLQMNSLKPEDTAVYYCNVNVGFEYW GQGTQVTVSSTSGKSYPTVSADYQDAVEKAKKKLRGFIAEKRCAPLMLRLAFHSAGTFDK GTKTGGPFGTIKHPAELAHSANNGLDIAVRLLEPLKAEFPILSYADFYQLAGVVAVEVTG GPKVPFHPGREDKPEPPPEGRLPDPTKGSDHLRDVFGKAMGLTDQDIVALSGGHTIGAAH KERSGFEGPWTSNPLIFDNSYFTELLSGEKEGLLQLPSDKALLSDPVFRPLVDKYAADED AFFADYAEAHQKLSELGFADAEFDYPYDVPDYAGAQPARSGGGLNDIFEAQKIEWHEGAL EHHHHHH
VHH-mCherry	MASMTGGQQMGRGSDQVQLVESGGALVQPGGSLRLSCAASGFPVNRYSMRWYRQAPGKER EWVAGMSSAGDRSSYEDSVKGRFTISRDDARNTVYLQMNSLKPEDTAVYYCNVNVGFEYW GQGTQVTVSSTSMVSKGEEDNMAIIKEFMRFKVHMEGSVNGHEFEIEGEGEGRPYEGTQT AKLKVTKGGPLPFAWDILSPQFMYGSKAYVKHPADIPDYLKLSFPEGFKWERVMNFEDGG VVTVTQDSSLQDGEFIYKVKLRGTNFPSDGPVMQKKTMGWEASSERMYPEDGALKGEIKQ RLKLKDGGHYDAEVKTTYKAKKPVQLPGAYNVNIKLDITSHNEDYTIVEQYERAEGRHST GGMDELYKEFDYPYDVPDYAGAQPARSGGGLNDIFEAQKIEWHEGALEHHHHHH

Table S2: Protein sequences of the EGFP-labeled reporter proteins.

EGFP in green, the receptor sequences in black with transmembrane segments and the N-terminal signal sequence of influenza virus hemagglutinin in yellow.

EGFP reporter	Protein sequence
EGFP	MVSKGEELFTGVVPILVELDGDVNGHKFSVSGEGEGDATYGKLTLKFICTTGKLPVPWPT LVTTLTYGVQCFSRYPDHMKQHDFFKSAMPEGYVQERTIFFKDDGNYKTRAEVKFEGDTL VNRIELKGIDFKEDGNILGHKLEYNYNSHNVYIMADKQKNGIKVNFKIRHNIEDGSVQLA DHYQQNTPIGDGPVLLPDNHYLSTQSALSKDPNEKRDHMVLLEFVTAAGITLGMDELYK
EGFP-CIMPR	MKTIIALSYIFCLVFARESMVSKGEELFTGVVPILVELDGDVNGHKFSVSGEGEGDATYG KLTLKFICTTGKLPVPWPTLVTTLTYGVQCFSRYPDHMKQHDFFKSAMPEGYVQERTIFF KDDGNYKTRAEVKFEGDTLVNRIELKGIDFKEDGNILGHKLEYNYNSHNVYIMADKQKNG IKVNFKIRHNIEDGSVQLADHYQQNTPIGDGPVLLPDNHYLSTQSALSKDPNEKRDHMVL LEFVTAAGITLGMDELYKSGLRSRAVGAVLSLLLVALTGCLLALLLHKKERRETVINKLT SCCRRSSGVSYKYSKVSKEEETDENETEWLMEEIQVPAPRLGKDGQENGHITTKAVKAEA LSSLHGDDQDSEDEVLTVPEVKVHSGRGAEVESSQPLRNPQRKVLKEREGERLGLVRGEK ARKGKFRPGQRKPTAPAKLVSFHDDSDEDLLHI
EGFP-CDMPR	MKTIIALSYIFCLVFARESMVSKGEELFTGVVPILVELDGDVNGHKFSVSGEGEGDATYG KLTLKFICTTGKLPVPWPTLVTTLTYGVQCFSRYPDHMKQHDFFKSAMPEGYVQERTIFF KDDGNYKTRAEVKFEGDTLVNRIELKGIDFKEDGNILGHKLEYNYNSHNVYIMADKQKNG IKVNFKIRHNIEDGSVQLADHYQQNTPIGDGPVLLPDNHYLSTQSALSKDPNEKRDHMVL LEFVTAAGITLGMDELYKGTTEEKSCDLVGEKDKESKNEVALLERLRPLFNKSFESTVGQ GSDTYSYIFRVCREASNHSSGAGLVQINKSNDKETVVGRINETHIFNGSNWIMLIYKGGD EYDNHCGKEQRRAVVMISCNRHTLAANFNPVSEERGKVQDCFYLFEMDSSLACSPEVSHL SVGSILLVIFASLVAVYIIGGFLYQRLVVGAKGMEQFPHLAFWQDLGNLVADGCDFVCRS KPRNVPAAYRGVGDDQLGEESEERDDHLLPM
EGFP-TGN46	MKTIIALSYIFCLVFARESMVSKGEELFTGVVPILVELDGDVNGHKFSVSGEGEGDATYG KLTLKFICTTGKLPVPWPTLVTTLTYGVQCFSRYPDHMKQHDFFKSAMPEGYVQERTIFF KDDGNYKTRAEVKFEGDTLVNRIELKGIDFKEDGNILGHKLEYNYNSHNVYIMADKQKNG IKVNFKIRHNIEDGSVQLADHYQQNTPIGDGPVLLPDNHYLSTQSALSKDPNEKRDHMVL LEFVTAAGITLGMDELYKGTATESVKQEDAGVRPSAGNVSTHPSLSQRPGGSTKSHPEPQ TPKDSPSKSSAEAQTPEDTPNKSGAEAKTQKDSSNKSGAEAKTQKGSTSKSGSEAQTTKD STSKSHPELQTPKDSTGKSGAEAQTPEDSPNRSGAEAKTQKDSPSKSGSEAQTTKDVPNK SGADGQTPKDGSSKSGAEDQTPKDVPNKSGAEKQTPKDGSNKSGAEEQGPIDGPSKSGAE EQTSKDSPNKVVPEQPSRKDHSKPISNPSDNKELPKADTNQLADKGKLSPHAFKTESGEE TDLISPPQEEVKSSEPTEDVEPKEAEDDDTGPEEGSPPKEEKEKMSGSASSENREGTLSD STGSEKDDLYPNGSGNGSAESSHFFAYLVTAAILVAVLYIAHHNKRKIIAFVLEGKRSKV TRRPKASDYQRLDQKS
TfR-EGFP	MMDQARSAFSNLFGGEPLSYTRFSLARQVDGDNSHVEMKLAVDEEENADNNTKANVTKPK RCSGSICYGTIAVIVFFLIGFMIGYLGYCKGVEPKTECERLAGTESPVREEPGEDFPAAR RLYWDDLKRKLSEKLDSTDFTSTIKLLNENSYVPREAGSQKDENLALYVENQFREFKLSK VWRDQHFVKIQVKDSAQNSVIIVDKNGRLVYLVENPGGYVAYSKAATVTGKLVHANFGTK KDFEDLYTPVNGSIVIVRAGKITFAEKVANAESLNAIGVLIYMDQTKFPIVNAELSFFGH AHLGTGDPYTPGFPSFNHTQFPPSRSSGLPNIPVQTISRAAAEKLFGNMEGDCPSDWKTD STCRMVTSESKNVKLTVSNVLKEIKILNIFGVIKGFVEPDHYVVVGAQRDAWGPGAAKSG VGTALLLKLAQMFSDMVLKDGFQPSRSIIFASWSAGDFGSVGATEWLEGYLSSLHLKAFT YINLDKAVLGTSNFKVSASPLLYTLIEKTMQNVKHPVTGQFLYQDSNWASKVEKLTLDNA AFPFLAYSGIPAVSFCFCEDTDYPYLGTTMDTYKELIERIPELNKVARAAAEVAGQFVIK LTHDVELNLDYERYNSQLLSFVRDLNQYRADIKEMGLSLQWLYSARGDFFRATSRLTTDF GNAEKTDRFVMKKLNDRVMRVEYHFLSPYVSPKESPFRHVFWGSGSHTLPALLENLKLRK QNNGAFNETLFRNQLALATWTIQGAANALSGDVWDIDNEFRTRIDMVSKGEELFTGVVPI LVELDGDVNGHKFSVSGEGEGDATYGKLTLKFICTTGKLPVPWPTLVTTLTYGVQCFSRY PDHMKQHDFFKSAMPEGYVQERTIFFKDDGNYKTRAEVKFEGDTLVNRIELKGIDFKEDG NILGHKLEYNYNSHNVYIMADKQKNGIKVNFKIRHNIEDGSVQLADHYQQNTPIGDGPVL LPDNHYLSTQSALSKDPNEKRDHMVLLEFVTAAGITLGMDELYK

Table S3: Protein sequences of Mitotrap and the recombinant γ-FKBP fusion protein.

Mitotrap: Signal and transmembrane domain of Tom70p in blue and yellow, FRB in red, 3xFLAG epitope in green, and linker sequences in black.

γ-FKBP (from 20): γ-adaptin subunit of AP-1 in purple, FKBP in gray, and the brain-specific α epitope sequence in pink.

Knocksideways constructs	Protein sequence
Mitotrap	MKSFITRNKTAILATVAATGTAIGAYYYYNQLQQDPPVATGTMASRILWHEMWHEGLEEA SRLYFGERNVKGMFEVLEPLHAMMERGPQTLKETSFNQAYGRDLMEAQEWCRKYMKSGNV KDLLQAWDLYYHVFRRISKSKLDYKDHDGDYKDHDIDYKDDDDK
γ-FKBP	MPAPIRLRELIRTIRTARTQAEEREMIQKECAAIRSSFREEDNTYRCRNVAKLLYMHMLG YPAHFGQLECLKLIASQKFTDKRIGYLGAMLLLDERQDVHLLMTNCIKNDLNHSTQFVQG LALCTLGCMGSSEMCRDLAGEVEKLLKTSNSYLRKKAALCAVHVIRKVPELMEMFLPATK NLLNEKNHGVLHTSVVLLTEMCERSPDMLAHFRKLVPQLVRILKNLIMSGYSPEHDVSGI SDPFLQVRILRLLRILGRNDDDSSEAMNDILAQVATNTETSKNVGNAILYETVLTIMDIK SESGLRVLAINILGRFLLNNDKNIRYVALTSLLKTVQTDHNAVQRHRSTIVDCLKDLDVS IKRRAMELSFALVNGNNIRGMMKELLYFLDSCEPEFKADCASGIFLAAEKYAPSKRWHID TIMRVLTTAGSYVRDDAVPNLIQLITNSVEMHAYTVQRLYKAILGDYSQQPLVQVAAWCI GEYGDLLVSGQCEEEEPIQVTEDEVLDILESVLISNMSTSVTRGYALTAIMKLSTRFTCT VNRIKKVVSIYGSSIDVELQQRAVEYNALFKKYDHMRSALLERMPVMEKVTTNGPSEIVQ TNGETEPAPLETKPPPSGPQPTSQANDLLDLLGGNDITPVIPTAPTSKPASAGGELLDLL GDITIDVNGGPEPAKNLYTMGVQVETISPGDGRTFPKRGQTCVVHYTGMLEDGKKFDSSR DRNKPFKFMLGKQEVIRGWEEGVAQMSVGQRAKLTISPDYAYGATGHPGIIPPHATLVFD VELLKLEGSIDLTELEPPAPESPMALLADPAPAADPGAPAAAPTPASVPQISQPPFLLDG LSSQPLFNDIAPGIPSITAYSKNGLKIEFTFERSNTNPSVTVITIQASNSTELDMTDFVF QAAVPKTFQLQLLSPSSSVVPAFNTGTITQVIKVLNPQKQQLRMRIKLTYNHKGSAMQDL AEVNNFPPQSWQ